# Multi-temporal monitoring of leaf area index of rice under different nitrogen treatments using UAV images

Xiaoyue Du[1,2], Liang Wan[1,2], Haiyan Cen[1,2,3], Shuobo Chen[1,2], Jiangpeng Zhu[1,2], Hongyan Wang[4], Yong He[1,2,3*]

(1. *College of Biosystems Engineering and Food Science, Zhejiang University, Hangzhou 310058, China*;
2. *Key Laboratory of Spectroscopy Sensing, Ministry of Agriculture and Rural Affairs, Hangzhou 310058, China*;
3. *State Key Laboratory of Modern Optical Instrumentation, Zhejiang University, Hangzhou 310027, China*;
4. *West Electronic Business Co., LTD, Yinchuan 750002, China*)

**Abstract:** Unmanned aerial vehicles (UAVs) remote sensing with advanced optical techniques has become a promising tool to monitor crop growth status. Although numerous studies have been conducted to assess crop growth using UAV-based image data, there still exists a challenge for achieving a satisfactory result. This study thus employed UAV-based RGB and multispectral (MS) imaging to estimate the leaf area index (LAI) of rice during the whole growth period. With five nitrogen (N) treatments during rice growth, an octo-rotor UAV was used to collect multi-temporal RGB and MS images of rice canopies. Vegetation indices (VIs) were then extracted from RGB and MS images. The prediction models for LAI were developed based on four machine learning methods including partial least squares regression (PLSR), support vector machine (SVM), random forest (RF), and extreme learning machine (ELM). The estimation performances of the models were also evaluated. The results showed that the ELM model with fusing the VIs from RGB and MS images achieved the best prediction result. The initial jointing, booting, heading and filling stages and the combination of all growth stages achieved a satisfactory prediction of LAI with the coefficient of determination ($R^2$) of 0.78, 0.45, 0.55, 0.64 and 0.70, respectively, which indicated that the initial jointing stage provided the best result for LAI prediction. Further, the performance of the model developed from the optimal VIs for LAI prediction was improved with the root mean square error of prediction (RMSEP) reduced by 18.5% at whole growth stages and decreased inconsistently at each individual growth stage. In summary, this study has demonstrated that fusion of UAV-based RGB and MS images has a great potential for rice LAI prediction.

**Keywords:** rice, LAI, RGB image, multispectral image, UAV, vegetation indices
**DOI:** 10.33440/j.ijpaa.20200301.57

**Citation:** Du X Y, Wan L, Cen H Y, Chen S B, Zhu J P, Wang H Y, He Y. Multi-temporal monitoring of leaf area index of rice under different nitrogen treatments using UAV images. Int J Precis Agric Aviat, 2020; 3(1): 7–12.

## 1 Introduction

Leaf area index (LAI) is a useful indicator for crop growth diagnosis[1], biomass estimation[2] and yield prediction[3,4] in precision agriculture. Rice is one of the leading food crops of the world, and timely and accurate monitoring of rice LAI could improve the fertilizer management and ensure world food security. Traditional methods for LAI measurements mainly rely on the destructive sampling and field survey. Although these methods can provide an accurate measurement of LAI within a specific range, they were costly and labor-intensive, especially for the data collection at a large field scale[5,6]. Therefore, it is essential to develop an efficient method to monitor LAI.

Extensive researches have been carried out using remote sensing techniques to estimate LAI at different growth stages. Spectral information obtained from multispectral or hyperspectral data were widely used for crop monitoring[7,8]. Wan et al.[9] used vegetation indices (VIs) including normalized green red difference index (NGRDI), red green ratio index (RGRI) and modified green red vegetation index (MGRVI) to estimate the flower number and obtained a good result with the coefficient of determination ($R^2$) of 0.95. Yue et al.[7] found that there was a high correlation between the ratio vegetation index (RVI) and LAI, and they also proved that a better estimation of crop height can be achieved by using multiple VIs compared with those using a single vegetable index.

Multispectral (MS) or hyperspectral (HS) images from satellite or unmanned aerial vehicle (UAV) platforms showed a great potential to estimate LAI of crop[9]. Bacour et al.[13] developed a LAI estimation model with the reflectance extracted from the satellite images, and the best result of estimating LAI was achieved with the root mean square error (RMSE) of 0.47. Jin et al.[14] estimated the LAI of winter wheat by using multi-temporal Huanjing-1A/B (spectral) and RADARSAT-2 (SAR), and the LAI estimation was improved by combing several spectral VIs (e.g. the

**Received date:** 2020-02-03 **Accepted date:** 2020-03-16
**Biographies: Xiaoyue Du**, M.S. student, research interests: UAV remote sensing, Email: xydu@zju.edu.cn; **Liang Wan**, PhD. student, research interests: UAV remote sensing and radiative transfer model, Email: liangwan@zju.edu.cn; **Haiyan Cen**, PhD, Professor, research interests: optical imaging-based plant phenotyping and UAV remote sensing, Email: hycen@zju.edu.cn; **Shuobo Chen**, PhD student, research interests: UAV remote sensing for plant phenotyping, Email: csb@zju.edu.cn; **Jiangpeng Zhu**, PhD student, research interests: UAV design and flight control system, Email: zhujianpn@zju.edu.cn; **Hongyan Wang**, President, research interests: agricultural internet of things, Email: nxwhy01@126.com.
*** Corresponding author: Yong He**, PhD, Professor, research interest: precision agriculture and agricultural aviation application, Email: yhe@zju.edu.cn.

enhanced vegetation index (EVI) and modified triangular vegetation index (MTVI2)) and radar polarimetric parameters (e.g. the radar vegetation index (RVI) and double-bounce eigenvalue relative difference (DERD)).

Compared with satellite-based remote sensing, the low-cost UAV remote sensing system has received much attention for crop growth monitoring[15-17]. Due to the flexibility and simplicity of operation and image processing, UAV remote sensing has shown a great potential for LAI estimation and practical applications in a small farmland[18]. Yue et al.[7] combined the VIs extracted from UAV images and the crop height to estimate LAI of winter wheat, and achieved the $R^2$ of 0.94 (RMSE = 0.33) and 0.58 (RMSE = 0.86) by using random forest (RF) and partial least squares regression (PLSR) methods, respectively. Kanning et al.[19] employed a UAV equipped with a hyperspectral camera to extract the canopy spectra, and achieved a good prediction result of wheat LAI based on the PLSR method with $R^2$ = 0.79 and RMSE = 0.18, respectively.

Although many studies have been performed by using UAV remote sensing to estimate LAI of different crops, they mostly focused on acquiring the data with a single imaging sensor. Several factors such as canopy structure, illumination condition, and growth stages could affect the data acquired from the UAV remote sensing platform. Therefore, this study was aimed to estimate the rice LAI by using UAV-based RGB and MS images at multiple growth stages, and the specific goals were to (1) investigate the LAI change during the whole growth period, (2) determine the optimal stage and VIs for LAI prediction of rice, and (3) select the best prediction model of rice LAI.

## 2 Materials and methods

### 2.1 Experimental design and LAI measurement

Rice was planted in Grain-production Functional Area of Anhua Town, Zhuji City, Zhejiang Province, China in early June, 2019 (29°31′5.35″N, 120°6′6.12″E). There were 100 plots with each of 9×5 $m^2$, and a protection lane with the width of 1 m was also provided around the experimental plots. Five nitrogen (N) treatments with N0, N1, N2, N3 and N4 of 0, 120, 240, 360 and 480 kg/ha, respectively, were applied in the form of urea in the transplanting, tillering and booting stages with the ratio of 4: 3: 3. The same phosphate (P = 120 kg/ha) and potash (K = 240 kg/ha) fertilizers were applied to all plots. Regular field management for the irrigation and weed control was carried out based on the regional standard. LAI was measured using the plant canopy analyzer (LAI-2200C, LI-COR Inc., NE, USA) as a ground truth. The experiment was conducted at the initial jointing, booting, heading and filling stages during July-October, 2019. UAV-based RGB and MS images and LAI were collected at the same experimental day.

### 2.2 UAV-based image acquisition

An octo-rotor UAV equipped with RGB and MS cameras was used to acquire images of rice. The diameter and the height of UAV is 1.1 m and 0.35 m, respectively, with the maximum payload of 8 kg. The RGB camera is the Sony NEX-7 micro single camera (Sony, Dugang District, TKY, Japan) with the spatial resolution of 6000 × 4000 pixels, and the MS camera (MQ022MG-CM, XIMEA, Munster, Germany) with a 16 mm fixed focus lens. The resolution of the MS camera is 409 × 216 pixels. Images were acquired at the flight altitude of 25 m with the 75% lateral overlap and 60% forward overlap. The weather was cloudless and windless. The exposure time was modified based on the illumination condition during the flight campaign. Rice multispectral images were first corrected for radiation consistency, and then stitched using Agisoft PhotoScan software (Agisoft LLC, St. Petersburg, Russia). Matching features of images were first detected and stitching were automatically conducted by the software. Figure 1 shows the MS and RGB ortho-images of rice at the experimental field.

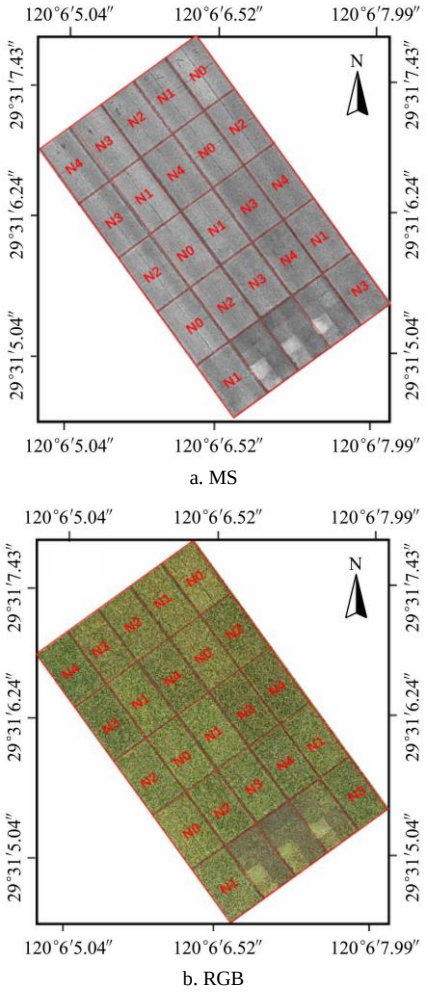


Figure 1 Ortho-images from multispectral (MS) and RGB camera

### 2.3 Selection of vegetation indices

Reflectance calibration was first conducted to convert digital numbers (DNs) of original MS images into the reflectance based on five calibration targets with the known reflectance[20]. Previous studies have demonstrated that various VIs extracted from RGB images (RGB-VIs) and multispectral images (MS-VIs) can used to evaluate the plant growth status[21]. Thus, we selected several commonly used VIs presented in Table 1 to estimate rice LAI. Based on visible and near-infrared bands, the normalized difference vegetation index (NDVI)[22] and ratio vegetation index (RVI)[23] were calculated from UAV-based MS images. In addition, the single-band reflectance from MS images was applied to estimate LAI. The VIs calculated from UAV-based RGB images mainly included the single-band DNs (R, G and B), single-band normalized DNs (r, g and b), excess green (EXG)[24], and visible-band difference vegetation index (VDVI)[25]. As shown in

Table 1, these VIs calculated from RGB and MS images have been proven to have the ability to estimate crop growth status. The correlation coefficient and the significance were compared to select the effective index with the best wavelength to achieve a higher prediction ability of LAI. The calculated VIs were the average reflectance of the corresponding sampling area in the image. The calculation formulas of various vegetation indices were shown in the following Table 1.

**Table 1 Vegetation indices (VIs) derived from MS and RGB images**

| Vegetation indices | Calculation | References |
|---|---|---|
| *MS-VIs* | | |
| Single band index | $R_\lambda$ | |
| Normalized difference vegetation index (NDVI) | (R796−R679)/(R796+R679) | [22] |
| Ratio vegetation index (RVI) | R796/R720 | [23] |
| Normalized difference red edge (NDRE) | (R790−R735)/(R790+R735) | [26] |
| Chlorophyll index (RedEdge) (CI) | R796/R732-1 | [27] |
| *RGB-VIs* | | |
| Single band index | R, G, B, r, g, b | |
| Excess green index (EXG) | 2*g−r−b | [24] |
| Visible-band difference vegetation index (VDVI) | (2*g−r−b)/(2*g+r+b) | [25] |
| Visible atmospherically resistant index (VARI) | (g−r)/(g+r−b) | [28] |

Note r=R/(R+G+B), g=G/(R+G+B), b=B/(R+G+B), R, G and B are the DNs of Red, Blue and Green channels, respectively. $R_\lambda$ represents the reflectance of a variable band in the spectral region of 600-1000 nm.

### 2.4 Model building and estimation of LAI

Different machine learning methods have been used to estimation crop growth status, but the prediction capacity for varied growth traits was different[29]. Therefore, in this study, four machine learning methods including PLSR, support vector machine (SVM), RF, and extreme learning machine (ELM) were compared to estimate the LAI based on the combinations of RGB-VIs and MS-VIs extracted from RGB and MS images at different growth stages.

PLSR is used to find the basic relationship between two matrices (X and Y), which can eliminate the multi-linear correlation to a certain extent. The essence of PLSR algorithm is based on the maximization of covariance. During the operation of the algorithm, the independent variable data matrix X and the dependent variable data matrix Y are decomposed at the same time, and the corresponding interpretations of hidden variables and response hidden variables are established. The regression equation between the two fully reflects the basic idea of PLSR.

SVM is a machine learning algorithm based on statistical learning and structural risk minimization, and has been widely used for solving classification and regression problems[30-32]. Support vector regression (SVR) is an important application branch in SVM[33]. The difference between SVR and SVM is that the SVR's essence is to find a plane and make the sum of the distances of all data in a set to the plane closest instead of finding the largest divergence like SVM.

RF is a parallel learner based on the decision tree. The algorithm does not require a large number of training samples and dynamic threshold settings. It can also perform a better vegetation treatment under complex lighting conditions (shadow and strong light). RF algorithm can reduce the overfitting phenomenon to a certain extent[34]. The main steps include constructing a training set, using set to generate a classification model, and then classifying all image pixels.

ELM has been proven to be a relatively novel learning algorithm for single-layer feedforward neural networks (SLFN)[35]. The ELM algorithm selects input weights and hidden biases randomly, and using the Moore-Penrose (MP) generalized to analyze the output weights. Compared with traditional gradient-based learning algorithms, ELM has advantages in terms of learning speed and generalization performance[35]. Meanwhile, it avoids many difficulties faced by gradient-based learning methods, such as stopping criteria, local minima, and the over-tuned problems.

When establishing estimation models, the dataset was divided into the training dataset (3/4) and the testing dataset (1/4), and ten-fold cross-validation was performed to reduce the modeling variability. The $R^2$ and the root mean square error of prediction (RMSEP) were used to evaluate model performance[36]. Higher $R^2$ and lower RMSEP indicate better estimation performance, and the RMSEP could be calculated as follows:

$$RMSEP = \sqrt{\frac{1}{n}\sum_1^n (p_i - \hat{p}_i)^2} \quad (1)$$

where, $p_i$ and $\hat{p}_i$ represents the measured and the predicted LAI, respectively.

## 3 Results and discussion

### 3.1 Variability of rice leaf area index

The LAI showed a similar change pattern among five N treatments at different growth stages, which increased from the initial jointing to the booting stage with a drop until the filling stage as shown in Figure 2. It can be seen that in each treatment of rice, the LAI at the initial jointing stage was the smallest, and reached the maximum at the booting stage. As for five N levels, the LAI showed an increasing tendency from N0 to N2, and then kept a relatively stable value from N2 to N4. The LAI at each growth stage of N4 was larger than the value of other treatments in the same period. N0 has the smallest LAI (2.018) throughout the growth period while the maximum value was 7.504 at N4 treatment. In addition, it is assumed that large-scale LAI differences at different stages of growth can cover most possible situations, which also makes it possible to test the ability of UAV remote sensing data for rice LAI estimation.

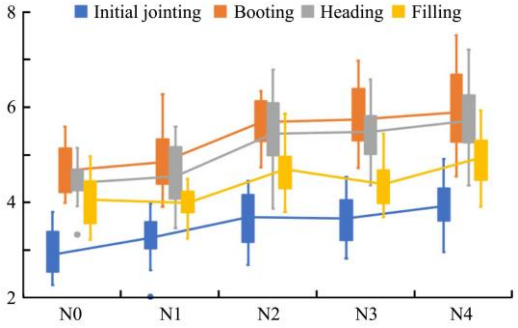


Figure 2 The changes of leaf area index (LAI) with varied nitrogen (N) treatments and growth stages

### 3.2 LAI prediction using UAV-based image data

The rice canopy spectra presented varied values at different growth stages. We first used the reflectance at the full wavelengths and VIs as the input of the algorithm first, and developed the prediction models using PLSR, SVM, RF and ELM, respectively. Four models presented different prediction accuracies of LAI as shown in Table 2. The ELM models developed from RGB-VIs and MS-VIs provided relative better results with the $R^2$ and RMSEP of 0.45 and 0.93, and 0.59 and 0.73, respectively. Compared with the result obtained from the single sensing data, the prediction performance was improved by fusion of RGB and MS image data with best result of $R^2$ = 0.70 and RMSEP = 0.54 from ELM. Therefore, ELM model was finally selected from the prediction of rice LAI.

**Table 2 Coefficient of determination ($R^2$) and the root mean square error of prediction (RMSEP) of different models for predicting LAI of rice**

| DATA SOURCE | Prediction models | | | | | | | |
|---|---|---|---|---|---|---|---|---|
| | PLSR | | SVM | | RF | | ELM | |
| | $R^2$ | RMSEP | $R^2$ | RMSEP | $R^2$ | RMSEP | $R^2$ | RMSEP |
| RGB-VIs | 0.18 | 2.24 | 0.14 | 1.35 | 0.32 | 0.62 | 0.45 | 0.93 |
| MS-VIs | 0.22 | 1.67 | 0.46 | 2.85 | 0.51 | 0.59 | 0.59 | 0.73 |
| FUSING (RGB & MS) | 0.27 | 1.84 | 0.57 | 0.80 | 0.67 | 0.60 | 0.70 | 0.54 |

### 3.3 LAI prediction accuracies at different growth stages

The growth status of rice at different growth stages is closely related to the final grain yield. To some extent, LAI can be used as a physiological index to predict the yield. Therefore, it is of great significance to develop a model with a high accuracy of LAI prediction at different stages. According to the research in Section 3.2, ELM model had advantages in predicting LAI of rice. Therefore, these models were used to predict LAI at different stages of rice, the results are shown in Figure 3.

From the Figure 3 and Table 2, it can be concluded that the initial jointing, booting, heading, filling and combining all growth stages achieved a satisfactory prediction of LAI. Meanwhile, ELM provided the best predictions at the initial jointing stage with the $R^2$ and RMSEP of 0.69 and 0.36, respectively, followed by the filling stage ($R^2$ = 0.60, RMSEP = 1.15). However, at the booting stage, the model of ELM's ability was relatively poor with $R^2$ and RMSEP of 0.45, 1.09, respectively. As a whole, ELM worked better at all stages with a relatively low RMSEP.

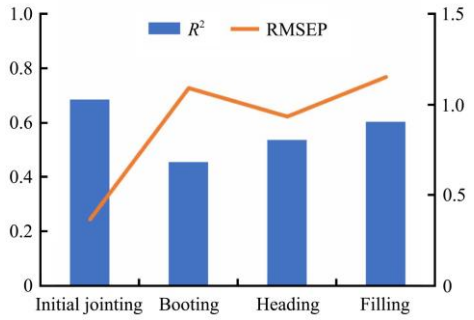


Figure 3 The Coefficient of determination ($R^2$) and the root mean square error of prediction (RMSEP) of LAI predict by ELM

### 3.4 LAI prediction using selected VIs

To reduce data redundancy and simplify modeling, five VIs calculated from RGB and MS images with the highest correlation to the LAI were selected based on the Pearson's correlation coefficient (Figure 4a). We also selected single bands that were highly correlated with LAI, including green, red, red edge and near-infrared bands as shown in Figure 4b. Finally, five VIs including RVI (796,720), NDRE (797,732), CI, EXG, VDVI and six individual bands at 624 nm, 632 nm, 674 nm, 679 nm, 732 nm and 838 nm were selected as the input of the prediction model.

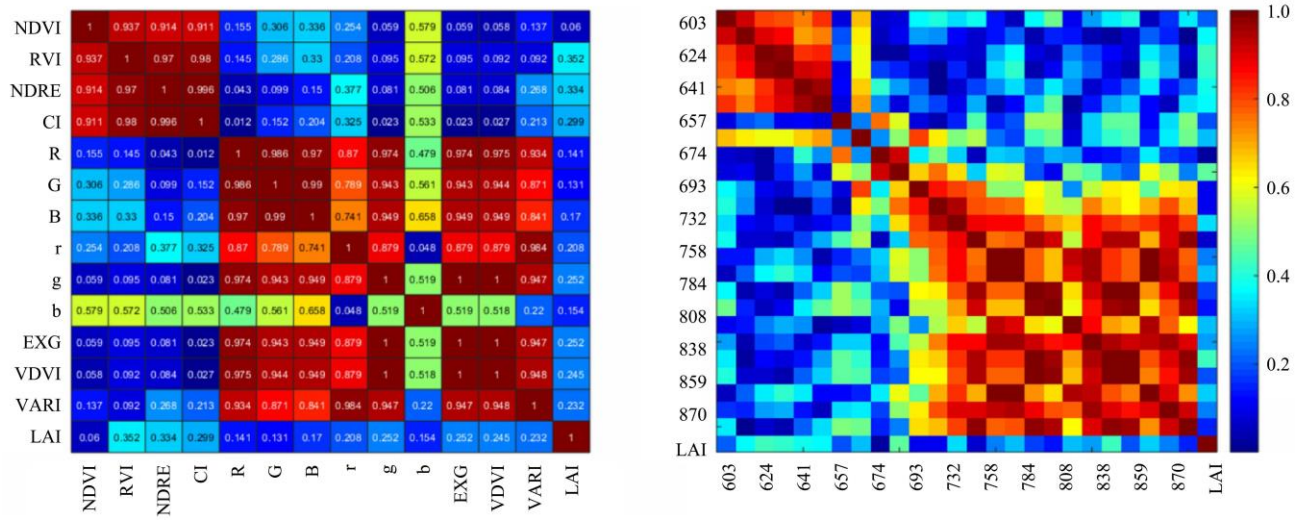


a. VIs b. single band

Figure 4 Correlation coefficient of VIs and single band with LAI

Compared with the ELM model of rice LAI in different stages, we can illustrate that based on the high correlation feature band and vegetation index as the input data, the prediction accuracies of rice LAI at different growth stages were improved except the booting stage with a slight decrease as shown in Figure 5. Compared with other growth stages, the model of ELM still obtained the highest $R^2$ at the initial jointing stage with an increase from 0.69 to 0.78, while RMSEP decreased from 0.36 to 0.28. The prediction accuracy for

LAI at the heading stage was significantly improved with the RMSEP greatly reduced. At the same time, compared to full-band input, $R^2$ and RMSEP from the filling stage was also improved with the $R^2$ increased from 0.60 to 0.64 and the RMSEP reduced from 1.15 to 0.22, respectively. The prediction result of the whole growth stage of rice LAI after selecting a special VIs as input is shown in Figure 6. The change of $R^2$ was not obvious, but at the same time RMSEP also showed a decreasing trend. Therefore, we can conclude that the method of using the band selected by correlation analysis as the model input can improve the prediction effect of rice LAI to a certain extent, and effectively reduced the RMSEP.

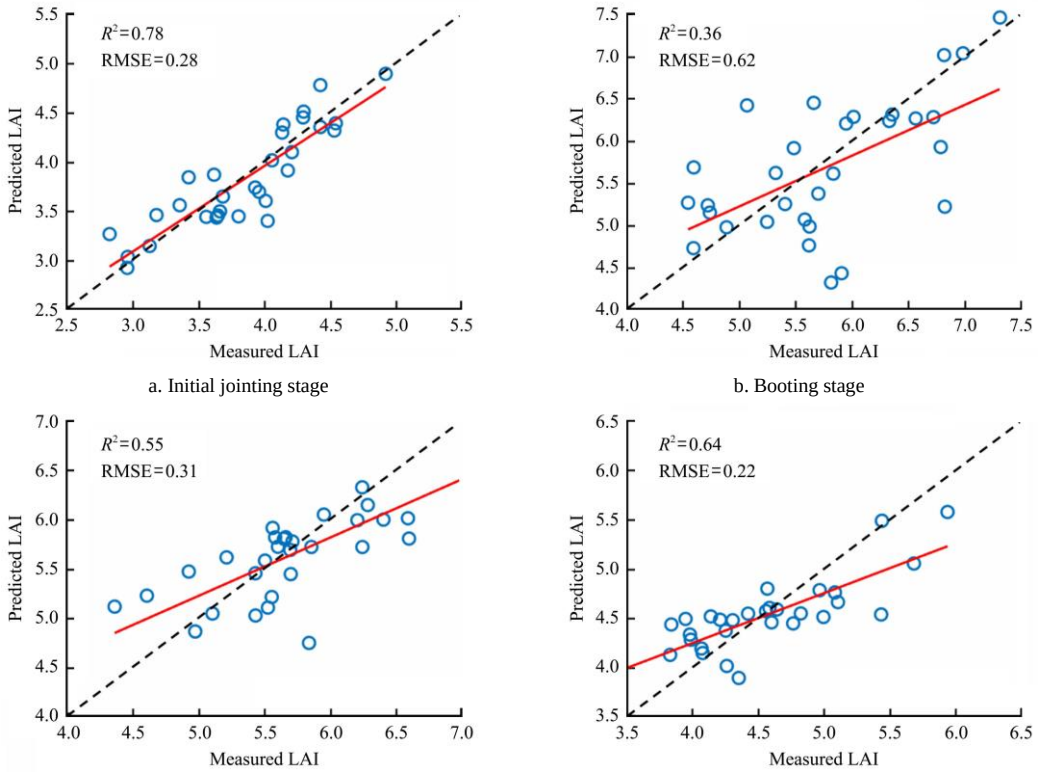


Figure 5 Prediction results of ELM model for each growing stage of rice

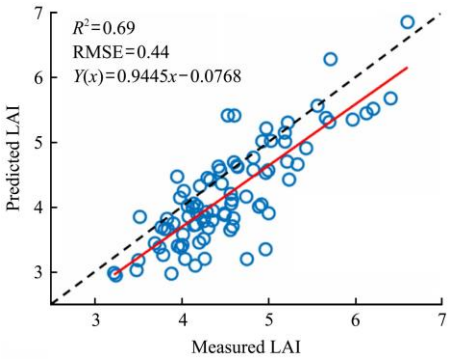


Figure 6 Prediction results of four models for all stages of rice

## 4 Conclusions

In this study, we explored the change of LAI with different N levels and growth stages. With the increase of N application, the LAI provided an increasing tendency. The varied growth stages also affected the changes of LAI, and the maximum LAI (7.504) was presented at the booting stage. Four machine learning methods including PLSR, SVM, RF and ELM were employed for LAI estimation, and they presented different prediction performances. With the comparison of four machine learning methods for LAI estimation over the entire period, the ELM model developed with all VIs extracted from RGB and MS images achieved the best prediction performance ($R^2$ = 0.70, RMSEP = 0.54). In addition, with the selection of the optimal VIs with the highest correlation to LAI, the model performance was improved with the RMSEP reduced to 0.44. The results showed that the ELM model with the input of six bands of remote sensing data and five VIs obtained the best prediction results of $R^2$ = 0.78 and RMSEP = 0.28 at the initial jointing stage. Overall, UAV-based RGB and MS image data achieved a satisfactory prediction of LAI for the four growth stages and the combination of all growth stages with the highest $R^2$ of 0.78, 0.45, 0.55, 0.64 and 0.70, respectively. This study demonstrated that the ELM model developed from UAV-based remote sensing image data has a great potential for LAI prediction of rice.

## Acknowledgments

This work was funded by the National Key R&D Program of China (2016YFD0200600, 2016YFD0200603), the Key Research & Development Program of Ningxia Hui Autonomous Region of China (2017BY067), and the National Natural Science Foundation of China (31801256). We also thank Liwen He and Jun Zhou for helping on UAV image data collection.

## [References]

[1] Jefferies R, Mackerron D. Responses of potato genotypes to drought. II. leaf area index, growth and yield. Annals of Applied Biology, 1993, 122(1): 105–112. doi: 10.1111/j.1744-7348.1993.tb04018.x.

[2] Cen H, Wan L, Zhu J, et al. Dynamic monitoring of biomass of rice under different nitrogen treatments using a lightweight UAV with dual image-frame snapshot cameras. Plant Methods, 2019, 15(1). doi: 10.1186/s13007-019-0418-8.

[3] Hasan M, Kamal A. Effect of fertilizer on grain yield and grain protein content of wheat. National Science Council of Sri Lanka, 1998, 26(1): 1–8. doi: 10.4038/jnsfsr.v26i1.3079.

[4] Duchemin B, Maisongrande P, Boulet G, et al. A simple algorithm for yield estimates: Evaluation for semi-arid irrigated winter wheat monitored with green leaf area index. Environmental Modelling and Software, 2008, 23(7): 876–892. doi: 10.1016/j.envsoft.2007.10.003.

[5] Li S, Ding X, Kuang Q, et al. Potential of UAV-based active sensing for monitoring rice leaf nitrogen status. Frontiers in Plant Science, 2018, 9, 1834. doi: 10.3389/fpls.2018.01834.

[6] Yao Y, Liu Q, Liu Q, et al. LAI retrieval and uncertainty evaluations for typical row-planted crops at different growth stages. Remote Sensing of Environment, 2008, 112(1): 94–106. doi: 10.1016/j.rse.2006.09.037.

[7] Yue J, Feng H, Jin X, et al. A comparison of crop parameters estimation using images from UAV-mounted snapshot hyperspectral sensor and high-definition digital camera. Remote Sensing, 2018, 10(7): 1138. doi: 10.3390/rs10071138.

[8] Xu X, Lu J, Zhang N, et al. Inversion of rice canopy chlorophyll content and leaf area index based on coupling of radiative transfer and Bayesian network models. ISPRS Journal of Photogrammetry and Remote Sensing, 2019, 150: 185–196. doi: 10.1016/j.isprsjprs.2019.02.013.

[9] Wan L, Li Y, Cen H, et al. Combining UAV-based vegetation indices and image classification to estimate flower number in oilseed rape. Remote Sensing, 2018, 10(9). doi: 10.3390/rs10091484.

[10] Li X, Zhang Y, Luo J, et al. Quantification winter wheat LAI with HJ-1CCD image features over multiple growing seasons. International Journal of Applied Earth Observation and Geoinformation, 2016, 44, 104–112. doi: 10.1016/j.jag.2015.08.004.

[11] Dong T, Liu J, Shang J, et al. Assessment of red-edge vegetation indices for crop leaf area index estimation. Remote Sensing of Environment, 2019, 222, 133–143. doi: 10.1016/j.rse.2018.12.032.

[12] Liang L, Di L, Zhang L, et al. Estimation of crop LAI using hyperspectral vegetation indices and a hybrid inversion method. Remote Sensing of Environment, 2015, 165: 123–134. doi: 10.1016/j.rse.2015.04.032.

[13] Bacour C, Baret F, Béal D, et al. Neural network estimation of LAI, fAPAR, fCover and LAI×Cab, from top of canopy MERIS reflectance data: Principles and validation. Remote Sensing of Environment, 2006, 105(4): 313–325. doi: 10.1016/j.rse.2006.07.014.

[14] Jin X, Yang G, Xu X, et al. Combined multi-temporal optical and radar parameters for estimating LAI and biomass in winter wheat using HJ and RADARSAR-2 data. Remote Sensing, 2015, 7(10): 13251–13272. doi: 10.3390/rs71013251.

[15] Verger A, Vigneau N, Chéron C, et al. Green area index from an unmanned aerial system over wheat and rapeseed crops. Remote Sensing of Environment, 2014, 152: 654–664. doi: 10.1016/j.rse.2014.06.006.

[16] MaitiniyaziMaimaitijiang, AbduwasitGhulam, PahedingSidike, et al. Unmanned aerial system (UAS)-based phenotyping of soybean using multi-sensor data fusion and extreme learning machine. ISPRS Journal of Photogrammetry and Remote Sensing, 2017, 134, 43–58. doi: 10.1016/j.isprsjprs.2017.10.011.

[17] Zhou X, Zheng H, Xu X, et al. Predicting grain yield in rice using multi-temporal vegetation indices from UAV-based multispectral and digital imagery. ISPRS Journal of Photogrammetry and Remote Sensing, 2017, 130: 246–255. doi: 10.1016/j.isprsjprs.2017.05.003.

[18] Lu N, Zhou J, Han Z, et al. Improved estimation of aboveground biomass in wheat from RGB imagery and point cloud data acquired with a low-cost unmanned aerial vehicle system. Plant Methods, 2019, 15(1). doi: 10.1186/s13007-019-0402-3.

[19] Kanning M, Kühling I, Trautz D, et al. High-resolution UAV-based hyperspectral imagery for LAI and chlorophyll estimations from wheat for yield prediction. Remote Sensing, 2018, 10(12). doi: 10.3390/rs10122000.

[20] Sona G, Pinto L, Pagliari D, et al. Experimental analysis of different software packages for orientation and digital surface modelling from UAV images. Earth Science Informatics, 2014, 7(2): 97–107. doi: 10.1007/s12145-013-0142-2.

[21] Duan B, Liu Y, Gong Y, et al. Remote estimation of rice LAI based on Fourier spectrum texture from UAV image. Plant Methods, 2019, 15(1): 1–12. doi: 10.1186/s13007-019-0507-8.

[22] Yi P, Zhu T, Li Y, et al. Remote prediction of yield based on LAI estimation in oilseed rape under different planting methods and nitrogen fertilizer applications. Agricultural & Forest Meteorology, 2019, 271: 116–125. doi: 10.1016/j.agrformet.2019.02.032.

[23] Jordan C F. Derivation of leaf-area index from quality of light on the forest floor. Ecology, 1969, 50(4): 663–666. doi: 10.2307/1936256.

[24] Woebbecke D, Meyer G, Bargen K, et al. Color indices for weed identification under various soil, residue, and lighting conditions. Transactions of the ASAE, 1995, 38(1): 259–269. doi: 10.13031/2013.27838.

[25] Wang Y, Zhang K, Tang C, et al. Estimation of rice growth parameters based on linear mixed-effect model using multispectral images from fixed-wing unmanned aerial vehicles. Remote sensing, 2019, 11, 1371. doi: 10.3390/rs11111371.

[26] Gitelson A, Merzlyak M. Quantitative estimation of chlorophyll-a using reflectance spectra: Experiments with autumn chestnut and maple leaves. Journal of Photochemistry and Photobiology. B: Biology, 1994, 22(3): 247–252. doi: 10.1016/1011-1344(93)06963-4.

[27] Li W, Niu Z, Chen H, et al. Remote estimation of canopy height and aboveground biomass of maize using high-resolution stereo images from a low-cost unmanned aerial vehicle system. Ecological Indicators, 2016, 67: 637–648. doi: 10.1016/j.ecolind.2016.03.036.

[28] Anatoly A, Yoram J, Robert S, et al. Novel algorithms for remote estimation of vegetation fraction. Remote Sensing of Environment, 2002, 80(1): 76–87. doi: 10.1016/s0034-4257(01)00289-9.

[29] Li S, Yuan F, Syed T, et al. Combining color indices and textures of UAV-based digital imagery for rice LAI estimation. Remote Sensing. 2019, 11, 1763. doi: 10.3390/rs11151763.

[30] Liu H, Zhang J, Pan Y, et al. An efficient approach based on UAV orthographic imagery to map paddy with support of field-level canopy height from point cloud data. IEEE Journal of Selected Topics in Applied Earth Observations and Remote Sensing, 2018: 1–13. doi: 10.1109/JSTARS.2018.2829218.

[31] Kwok T Y. Support vector mixture for classification and regression problems. 2000, 1: 255–258 vol.1. doi: 10.1109/ICPR.1998.711129.

[32] Dai J, Zhang G, Guo P, et al. Classification method of main crops in northern Xinjiang based on UAV visible waveband images. Transactions of the Chinese Society of Agricultural Engineering, 2018, 34(18): 130–137. doi: CNKI:SUN:NYGU.0.2018-18-015.

[33] Kaya G T. A hybrid model for classification of remote sensing images with linear SVM and support vector selection and adaptation. IEEE Journal of Selected Topics in Applied Earth Observations &Remote Sensing, 2013, 6(4): 1988–1997. doi: 10.1109/JSTARS.2012.2233463.

[34] Ham J, Chen Y, Crawford M, et al. Investigation of the random forest framework for classification of hyperspectral data. IEEE Transactions on Geoscience & Remote Sensing, 2005, 43(3): 492–501. doi: 10.1109/tgrs.2004.842481.

[35] Huang G, Zhou H, Ding X, et al. Extreme learning aachine for regression and multiclass classification. IEEE Transactions on Systems, Man and Cybernetics, Part B (Cybernetics), 2012, 42(2): 513–529. doi: 10.1109/tsmcb.2011.2168604.

[36] Gitelson A, Keydan G, Merzlyak M. Three-band model for noninvasive estimation of chlorophyll, carotenoids, and anthocyanin contents in higher plant leaves. Geophysical Research Letters, 2006, 33(11): L11402. doi: 10.1029/2006gl026457.